Mutual Diffusion in Compatible Polymer Blends

J. Kanetakis and G. Fytas*

Research Center of Crete, PO Box 1527, 711 10 Heraklio, Crete, Greece.
Received November 29, 1988; Revised Manuscript Received February 1, 1989

ABSTRACT: Dynamic light scattering has been employed for the study of diffusional dynamics in the compatible polymer blend poly(ethylene oxide) (PEO)/poly(propylene oxide) (PPO). Measurements of the static structure factor $S(q)$ at a scattering vector q and mutual diffusion coefficient D are reported for a series of molecular weights of PEO of 600, 1000, 2000, 4000, 18 000, and 62 000 covering the range from the Rouse regime to the well-entangled region for various volume fractions φ of PEO in the temperature range 70–100 °C. The molecular weight of PPO was kept constant at 1025. The present polymer mixture exhibits upper critical solution temperature and shows strong evidence of a composition-independent glass transition temperature, as supported by shear viscosity measurements. In the blend PEO(1000)/PPO(1025), D is severely reduced near the middle of the composition range due to the effect of thermodynamic interactions between the different chains. With the light-scattering technique we have been able to measure simultaneously D and $S(q)$ and extract the transport coefficient D^0 and the Flory–Huggins interaction parameter χ_F. At constant φ, D^0 is rather insensitive to changes in molecular weight of PEO in agreement with the "fast mode" theory. However, the φ dependence of D^0 in PEO(1000)/PPO(1025) blends does not agree with either the "fast" or "slow" mode theory, and the maximum it depicts near the middle of the composition range is not explainable by current theory. With a positive interaction parameter χ_F calculated for these blends, the mutual diffusion D (which is a weighted average of the tracer diffusivities of the two components) is found to be smaller than D^0. We have used the values of self-diffusion coefficients supplied by pulsed-field-gradient NMR spectroscopy to calculate D as a function of φ; a fairly reasonable agreement was then found between the experimental and calculated values of D.

Introduction

The diffusional dynamics of homogeneous polymer blends, aside from their practical relevance, are of current theoretical and experimental interest. In a binary mixture of interacting chemically different macromolecules A and B the thermal concentration fluctuations $\varphi_A(q)$ and $\varphi_B(q)$ determine the intensity in a scattering experiment. If the blend can be considered incompressible, $\varphi_A(q) = -\varphi_B(q)$, the mean-field theory gives the simplified expression for the dynamic structure factor[1-3]

$$S(q,t) = \langle \varphi_q(t)\, \varphi_{-q}(0) \rangle = S(q) \exp(-Dq^2t) \qquad (1)$$

where $S(q) = \langle |\varphi_q(0)|^2 \rangle$ is the static structure factor with $|\varphi_q(0)|^2$ being the Fourier transform of the mean-square concentration fluctuations. The factor $S(q)$ is related to the scattering power of the noninteracting coils and the Flory–Huggins interaction parameter χ_F by

$$1/S(q) = 1/S_A^0(q) + 1/S_B^0(q) - 2\chi_F \qquad (2)$$

For small q, eq 2 can be written in the form

$$1/S(q) = 2(\chi_S - \chi_F) + q^2l^2 \qquad (3)$$

where l is an effective monomer length[3] of the order of few angstroms.[4] In the $q \to 0$ limit the structure factor $S(q=0)$

$$1/S(0) = 2(\chi_S - \chi_F) \qquad (4)$$

diverges as the spinodal curve at which $\chi_S = \chi_F$ is approached from the homogeneous phase.

The mutual diffusion D in eq 1 which is affected by bare-chain mobilities and thermodynamic interactions is given by[1-3,5-7]

$$D = 2D^0(\chi_S - \chi_F)\varphi(1 - \varphi) \qquad (5)$$

where φ is the average volume fraction of one component and D^0, a transport coefficient, is a weighted average of the tracer diffusivities D_A^0 and D_B^0 in the blend. D^0 is in dispute between the different theoretical approaches. In the regime $qR_g \ll 1$ (R_g being the radius of gyration) the mean-field result reads[2,3,5]

$$1/D^0 = \varphi_B/(D_A^0N_A) + \varphi_A/(D_B^0N_B) \qquad (6)$$

In contrast to this result, other treatments[6,7] lead to the form

$$D^0 = \varphi_B(D_A^0N_A) + \varphi_A(D_B^0N_B) \qquad (7)$$

In all theoretical treatments so far, D_A^0 and D_B^0 are assumed to be independent of blend composition and similar to those of the bare chains. This further implies either that the glass transition temperature of the mixture $T_g(\varphi)$ is insensitive to its composition or that the measurements are performed at temperatures sufficiently higher than T_g.

On the experimental side, the techniques of dynamic light scattering,[8-11] forward recoil spectrometry (FRES),[12-14] and infrared microdensitometry[15] have been employed to study the mutual diffusion in compatible blends of chemically dissimilar polymers[8-13] and isotopic polymers.[14,15] While the first technique probes the concentration fluctuations (eq 1) at equilibrium, the other two techniques require a built-in concentration gradient. The experimental work done so far is quite limited,[16] and the current evidence is still inconclusive. To test rigorously the theoretical results, besides the main measurements of $D(\varphi,N)$, knowledge of $D_A^0(\varphi,N)$, $D_B^0(\varphi,N)$, and the interaction parameter $\chi_F(\varphi)$ is required as a function of composition φ and degree of polymerization N. In particular, the interpretation of the experimental $D(\varphi)$ needs careful consideration owing to the variation of T_g with composition.[9,12] This introduces another major dependence on concentration in addition to those predicted by eq 6 and 7. A method to deal with this problem was examined in a light-scattering study on the binary blend polystyrene/poly(phenylmethylsiloxane).[9]

There is more consensus on the role of the thermodynamic factor $\chi_S - \chi_F$ in eq 5. Reduced mutual diffusion ($D < D^0$) was reported for the polymer blend poly(ethylene oxide)/poly(propylene oxide)[10] (PEO/PPO) and for the mixture of normal and deuterated polystyrene[14] with $\chi_F > 0$, by using light scattering and forward recoil spectrometry, respectively. In both cases a "thermodynamic slowing down" effect was observed as χ_F approaches χ_S. On the other hand, enhanced mutual diffusivity, $D > D^0$, was reported for the mixture polystyrene/poly(xylenyl ether)[12] (PS/PXE) due to favorable segment–segment interactions ($\chi_F < 0$). Another, rather strigent prediction of both eq 6 and 7 is that D^0 becomes molecular weight independent for unentangled Rouse chains, i.e., $D_i^0 \propto N_i^{-1}$

0024-9297/89/2222-3452$01.50/0 © 1989 American Chemical Society

(i = A, B). This striking result has recently been confirmed for the PEO/PPO blend[11] by using a dynamic light-scattering experiment to obtain both D and $S(0)$. For the compatible mixture PS/PXE at $\varphi_{PS} = 0.55$ in the entangled regime the measured length chain dependence of D can be reconciled only by eq 7, which predicts domination of the faster moving chain.[13] A similar conclusion emerged from a more recent investigation of the broadening of the concentration profile between two saturated polybutadienes differing in their molecular weight by means of infrared densitometry.[15] However, a similar X-ray study on polyvinylidene/poly(methyl methacrylate)[17] has favored the "parallel" addition or the "slow mode" theory (eq 6). A direct concentration-dependent study of D employed in blends of chemically different components to discriminate between eq 6 and 7 usually suffers from the strongly composition dependent $T_g(\varphi)$.[9,12] The present paper is concerned with the effect of temperature, molecular weight, and composition dependence of D in PEO/PPO mixtures in the homogeneous phase. There is a strong evidence that T_g is insensitive to blend composition, and in addition the measurements are performed at temperatures far above T_g. This considerably facilitates the analysis of the data taken at different concentrations and temperatures, therefore yielding more convincing results. The photon correlation spectroscopic technique was carefully employed to obtain both the mutual diffusion D and the static structure factor S.[9,18] The self-diffusion coefficients of the two components were measured by using pulsed-field-gradient NMR spectroscopy.[19]

Experimental Section

Photon Correlation Spectroscopy. The correlation functions $G(q,t)$ of the light-scattered intensity of the homogeneous blends were measured at different temperatures (70–100 °C) and at a scattering angle of $\theta = 90°$. The diffusional character of the blends dynamics was checked by measuring the relaxation rate at various angles (45°, 90°, 150°). The light source was an argon ion laser (Spectra Physics 2020) operating at 488 nm, single mode, with a power of 200 mW. The incident beam was polarized vertically with respect to the scattering plane, and no polarizer was used for the scattered light since both of the blend components are predominantly isotropic scatterers. The light intensity correlation functions over 4.3 decades in time were measured with a 28-channel logarithmic–linear single clipped correlator (Malvern K7027) in one run. In the homodyne limit the desired normalized correlation function $g(q,t)$ of the scattered electric field is related to $G(q,t)$ by

$$G(g,t) = A\left[1 + f\frac{1+k}{1+\langle n\rangle}\left|\alpha g(q,t)\right|^2\right] \quad (8)$$

where A is the base line, $\langle n\rangle$ is the average number of photocounts per sampling interval, k is the clipping level, and f is the instrumental factor. The factor α is the fraction $I_\varphi(q)/I(q)$ of the scattered intensity arising from concentration fluctuations. In this case, $g(q,t)$ is identified with

$$g(q,t) = S(q,t)/S(q) \quad (9)$$

In our photon correlation spectroscopy experiments besides the correlation function due to concentration fluctuations, we occasionally observed a second correlation function at very long delay times that occurred long after the first one had already decayed off. Although its existence is taken into account in the fitting procedure, the physical origin of this slow (as compared to the correlation function strictly due to concentration fluctuations) process has not been yet rationalized. It is worthwhile mentioning that this slow mode does not show up at the correlograms of the pure components. Figure 1 shows a typical semilog plot of the unnormalized time correlation function $C(q,t) = \alpha g(q,t)$ of the bulk component PPO (bottom) and of a homogeneous blend with different volume fractions of PEO (top). The flat featureless form of the homopolymer data demonstrates the absence of density fluctuations in the time range under consideration. The unique feature of the amorphous blend, as compared to the pure homopolymers, is nicely depicted.

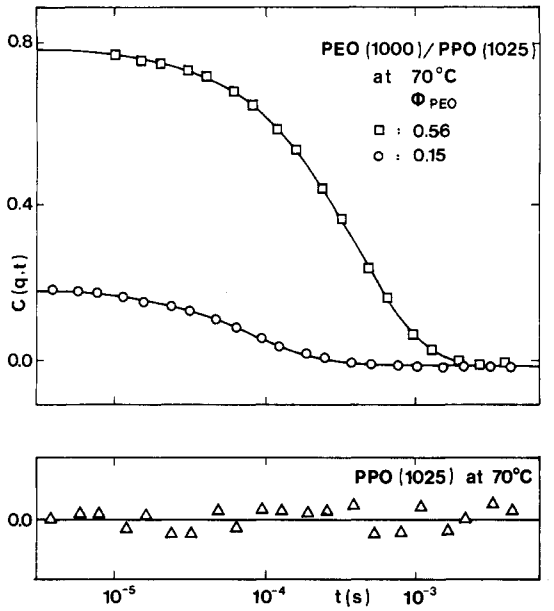

Figure 1. Lower curve: Autocorrelation function for the pure poly(propylene oxide) with molecular weight 1025. Upper curve: Concentration autocorrelation function ($C(q,t) = \alpha g(q,t)$) for a mixture of poly(ethylene oxide) and poly(propylene oxide) with molecular weights 1000 and 1025, respectively, at two different volume fractions φ_{PEO}. Solid lines represent single-exponential fits.

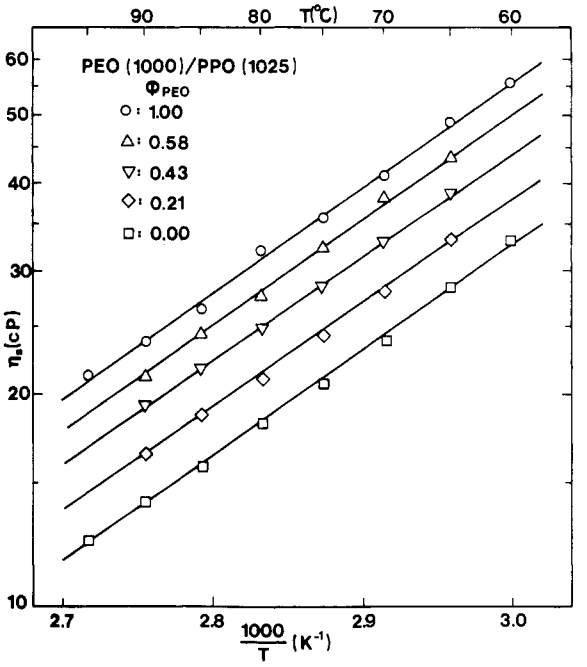

Figure 2. Shear viscosity η_S versus temperature for the pure homopolymers PEO(1000) and PPO(1025) and three homopolymer blends PEO(1000)/PPO(1025) with different volume fractions of PEO(1000). Solid lines are fits to the Arrhenius equation.

Materials. The polymer mixture we employ in our study, PEO/PPO, was chosen mainly for two reasons. First the temperature of the measurements is far enough from the glass transition temperature, T_g, of the components[20] as evidenced by the Arrhenius-type dependence of shear viscosity η_s on temperature T in Figure 2. Therefore, the semiempirical WLF relation based on the $(T - T_g)$ difference does not need to be employed. Moreover, the microscopic friction coefficient is virtually composition independent, as can be seen from the constant value of

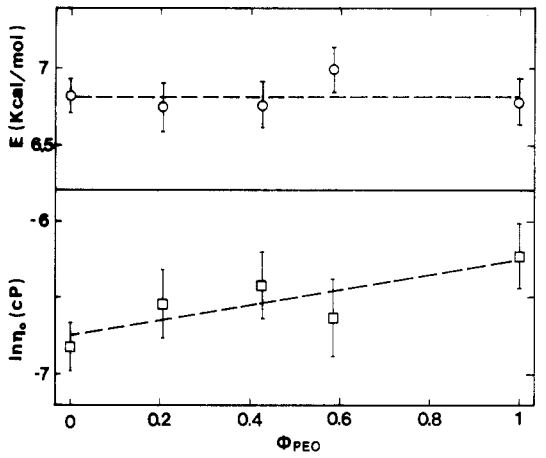

Figure 3. Activation energy E and ln η_0 (as extracted from the Arrhenius equation of shear viscosity versus temperature, Figure 2) plotted as functions of the volume fraction of PEO for the pure homopolymers PEO(1000) and PPO(1025) and three blends PEO(1000)/PPO(1025). Compositions φ_{PEO} are the same as in Figure 2. Dashed lines are linear least-squares fits to the data.

the activation energy E with volume fraction of PEO in Figure 3. These characteristics of the PEO/PPO compatible blend constitute a great advantage over some recently studied polymer blends[8,12] where a strongly composition-dependent T_g complicates the analysis. On the contrary, the present polymer blend renders the analysis of the D values straightforward.

Six mixtures were employed with molecular weight of PPO, M_{PPO} = 1025, and molecular weights of PEO 600, 1000, 2000, 4000, 18000 and 62000. The low molecular weight samples (up to 4000) were purchased from Merck, Ferak and Serva (West Germany) and the PEO samples with molecular weights 18000 and 62000 were kindly donated by Prof. Eisenach, Karlsruhe (West Germany).

The samples with narrow molecular weight distributions and without further fractionation were dissolved in dry benzene, filtered through 0.2-μm Millipore filters directly into the scattering cells, and kept for several days at 80 °C under vacuum. The dust-free amorphous polymer blends were transparent and optically homogeneous above about 60 °C. The mixture exhibits convenient upper critical solution temperature (UCST).[21]

Data Analysis

The net experimental intensity autocorrelation function $[G(q,t)/A - 1]^{1/2}$ with fixed base line A has been fitted by a single-exponential decay function for $g(q,t)$ such that

$$[G(q,t)/A - 1]^{1/2} = b \exp(-t/\tau) \qquad (10)$$

A nonlinear least-squares routine has been employed to obtain the values of the amplitude $b = [f(1 + k)/(1 + \langle n \rangle]^{1/2}\alpha$ and relaxation time τ. Originally we fitted the function $[G(q,t)/A - 1]^{1/2}$ with a fractional exponential decay function $b \exp[-(t/\tau)^{\beta}]$ and we found β to be very close to unity, henceforth we decided to use a single-exponential decay function as practically adequate (eq 1).

A crucial test of the theory is the q dependence of the relaxation rate Γ ($=\tau^{-1}$). The results at different scattering angles at 75 °C are shown in Figure 4 for a PEO(1000)/PPO(1025) mixture with PEO volume fraction φ = 0.39. This figure demonstrates clearly the diffusional character of the observed relaxation process as predicted theoretically in the regime $qR_g \ll 1$. This experimental verification justifies the use of the simple formula

$$D = 1/(\tau q^2) \qquad (11)$$

to calculate the mutual diffusion coefficient D from the relaxation time τ and the magnitude of the scattering vector $q = (4\pi n/\lambda) \sin(\theta/2)$, where n, λ, and θ are, respectively, sample refractive index, incident beam wavelength, and scattering angle.

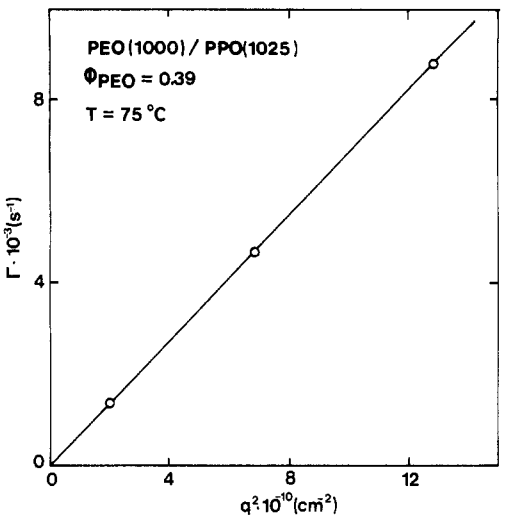

Figure 4. Relaxation rate Γ as a function of q^2, q being the magnitude of the scattering vector, for a homopolymer blend PEO(1000)/PPO(1025).

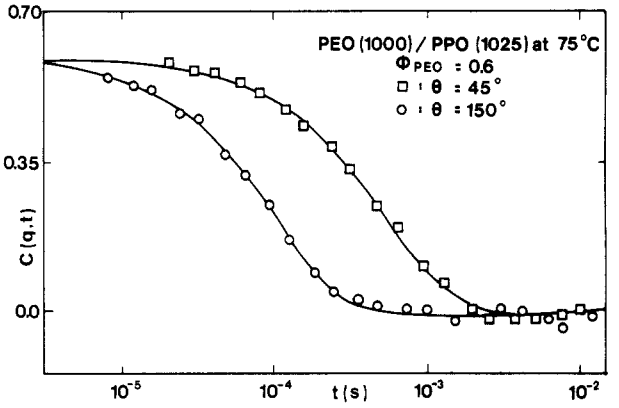

Figure 5. Concentration autocorrelation function for a homopolymer blend PEO(1000)/PPO(1025) at two scattering angles. Solid lines represent single-exponential fits.

The static structure factor $S(q)$ can be obtained from the Rayleigh ratio $R(q)$ due to concentration fluctuations:

$$S(q) = R(q)\lambda^4\rho/[4\pi^2 n^2(\partial n/\partial\varphi)^2] \qquad (12)$$

where ρ is the number density, n is the blend refractive index, $\partial n/\partial\varphi$ is the refractive index increment, and $R(q)$ is given by

$$R(q) = (I_\varphi(q)/I_t)(n/n_t)^2 R_t \qquad (13)$$

where $I_\varphi(q) = \alpha I(q)$ is scattered light intensity due to concentration fluctuations; I_t, n_t, and R_t are for toluene static intensity measured at the same experimental conditions as $I_\varphi(q)$, refractive index, and absolute Rayleigh ratio, respectively.

There is a good agreement between $I_\varphi(q)$ as calculated via the parameter b and the expression

$$I_\varphi(q) = I(q) - (\varphi_A I_A + \varphi_B I_B) \qquad (14)$$

where the contribution of the density fluctuations I_A and I_B of the separate components to the scattered light intensity has been subtracted from the total scattered intensity to yield $I_\varphi(q)$ due directly to concentration fluctuations.

Figure 5 shows two net correlation functions of a PEO(1000)/PPO(1025) blend with volume fraction of PEO, φ_{PEO} = 0.6, taken at different scattering angles. Owing to the angular dependence of the relaxation time, the cor-

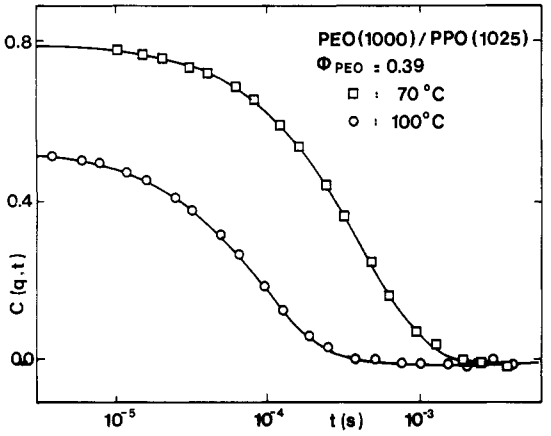

Figure 6. Concentration autocorrelation function for a homopolymer blend PEO(1000)/PPO(1025) at two temperatures. Solid lines represent single-exponential fits.

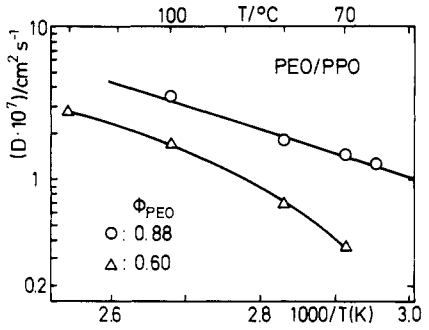

Figure 7. Measured mutual diffusion coefficient D plotted as a function of temperature for PEO(1000)/PPO(1025) blends with different volume fractions φ_{PEO}.

relation function at $\theta = 45°$ decays with a slower rate than the one at $\theta = 150°$. However, the two correlation functions have a common intercept α, which implies that the static structure factor $S(q)$ is virtually q independent in the $q \to 0$ limit. It further denotes that $q^2l^2S(0) \ll 1$ and henceforward $S(q) = S(0)$.

Results and Discussion

Temperature Dependence. According to eq 5 the variation of the mutual diffusion D with temperature must be accounted for by the temperature dependence of the mobility D^0 and the thermodynamic factor $S(0)$. The former should exhibit an Arrhenius temperature dependence similar to that observed for the shear viscosities (Figures 2 and 3). On the other hand, the variation of the structure factor $S(0)$ with temperature can become important only for temperatures close to the coexistence curve (i.e., $\chi_F \sim \chi_S$). In this case the amplitude of the correlation function changes significantly with temperature as shown in Figure 6 for the PEO/PPO mixture with φ near the middle of the blend composition range. At extreme compositions, where $\chi_s \gg \chi_F$,[18] $S(0)$ is a weak function of temperature and therefore the temperature dependence of D is expected to be different for different blend compositions. This situation is depicted in Figure 7 for the PEO/PPO mixture at two different compositions. The thermodynamic "slowing down" effect[10,14,22] is evident for the mixture with $\varphi = 0.6$. Alternatively, the diffusion data for $\varphi = 0.88$ exhibit an Arrhenius temperature dependence:

$$D = D_0 \exp[-E/RT] \qquad (15)$$

with activation energy $E = 7 \pm 0.2$ kcal/mol and $D_0 = 5.98 \times 10^{-3}$ cm^2/s. The E value is very close to that obtained from the temperature dependence of the shear viscosity

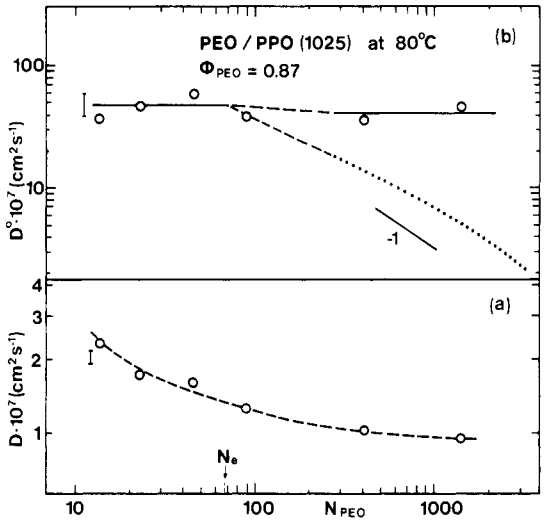

Figure 8. (a) Measured mutual diffusion coefficient D versus degree of polymerization N_{PEO} of the PEO component, at 80 °C with constant molecular weight of PPO. (b) Transport coefficient D^0 plotted as a function of N_{PEO}, under the same conditions as in (a). For $N_{PEO} < N_e$, the solid line is an average D^0 from the experimental points. For $N_{PEO} > 4N_e$, the dotted and solid lines represent respectively eq 6 and 7. For $N_e < N_{PEO} < 4N_e$ (dashed line) the reptation model by itself cannot describe diffusion in the entangled PEO matrix. For more details see text.

data (Figure 3). The temperature dependence of the mutual diffusion in dilute PEO/PPO blends is therefore determined by the mobility D^0 term.

Molecular Weight Dependence. In all theoretical treatments of mutual diffusion the Onsager transport coefficient $\Omega = D^0\varphi(1 - \varphi)$ (eq 5) for unentangled "Rouse" chains is expected (eq 6 and 7) to be independent of molecular weight. Alternatively, the composite mutual diffusion D may vary with molecular weight of the blend components;[23] however this change can be accounted for by the variation of the thermodynamic term (eq 5) with molecular weight.[11,24] In a previous short paper[11] we demonstrated that in PEO/PPO ($\varphi_{PEO} = 0.87$) mixtures with $M_{PPO} = 1025$ and $M_{PEO} = 600$, 1000, and 2000, the transport coefficient Ω was virtually independent of the chain length of PEO. The entanglement molecular weight M_c of bulk PEO is about 3000[25] (from diffusion measurements).

In this work, we increase the M_{PEO} above its entanglement value (M_c/φ_{PEO}) in the PEO/PPO blend containing a volume fraction $\varphi_{PEO} = 0.87$. The coefficient D at 80 °C is plotted in Figure 8 as a function of N_{PEO}, the degree of polymerization of PEO. As seen in Figure 8a, D decreases monotonically as N_{PEO} increases above its entanglement value. Most of this reduction arises from the structure factor $S(0)$. In fact, the latter was found to be an increasing function of N_{PEO}, whereas the transport coefficient D^0 shows a much lesser molecular weight dependence (Figure 8b).

From the proposed expressions for D^0, eq 6 predicts domination of the slower moving component whereas eq 7 implies that the fast moving component controls interdiffusion at constant φ. These predictions will be compared quantitatively with the values of D^0 in Figure 8b at least in the highly entangled PEO matrix. In computing D^0 (eq 6 and 7), we used

$$D_A^0 = {}^4/_{15} w_A N_e / N_A^2, \quad D_B^0 = w_B / N_B \qquad (16)$$

for the tracer diffusion coefficient of the entangled PEO (≡A) and unentangled PPO (≡B) chains and entanglement degree of polymerization of PEO, $N_e = 78$. For the former

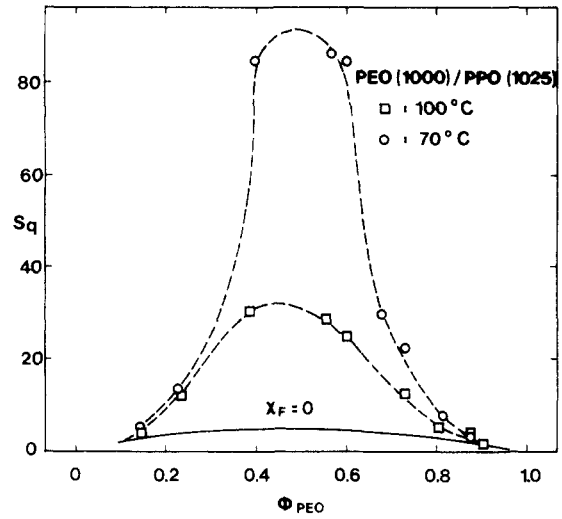

Figure 9. Static structure factor $S(q)$ plotted as a function of composition φ_{PEO} for PEO(1000)/PPO(1025) homopolymer blends at different temperatures. For comparison the calculated structure factor $S(q)$ with $\chi_F = 0$ is also plotted. Dashed lines are to guide the eye.

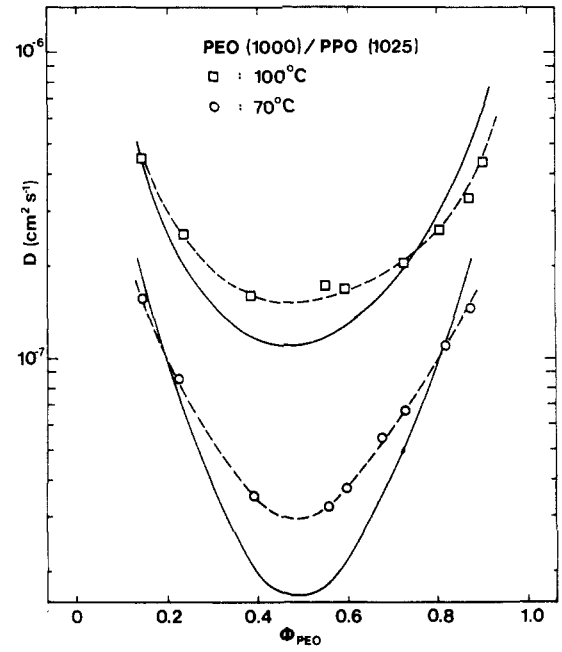

Figure 10. Measured mutual diffusion coefficient D plotted as a function of composition φ_{PEO} in PEO(1000)/PPO(1025) blends at 100 °C (□) and 70 °C (○). Dashed lines are drawn as a guide through the experimental data. Solid lines are the calculated D via eq 4, 5, and 7 by inserting the values of the static structure factor $S(0)$ from Figure 9 and employing for D_A^0 and D_B^0 the self-diffusivities D_A^* and D_B^* of PEO(1000) and PPO(1025) as measured by pulsed-field-gradient NMR.[19] Since the self-diffusivities of PEO(1000) and PPO(1025) are quite similar, the solid lines can be considered to be valid for both the "fast" and "slow" mode theories.

we assumed the validity of the reptation model[26] for molecular weights of PEO greater than 4 times its entanglement molecular weight.[32] Furthermore, the microscopic mobilities w_A and w_B are set equal to the value of D^0 in the unentangled PEO/PPO mixture, i.e., for molecular weights of PEO, $M_{PEO} < 3500$. The dotted and solid lines in Figure 8b show, respectively, the D^0 computed by using eq 6 and 7. Clearly the variation of D^0 with $N_{PEO} > N_e$ is in good agreement with the prediction of the fast theory (eq 7). The transport coefficient D^0 is controlled by the unentangled PPO chains whose molecular weight remains constant. A similar conclusion was drawn from a recent FRES study of mutual diffusion in entangled PS/PXE blends,[13,22] in which the interdiffusion D at $\varphi_{PS} = 0.55$ was measured as function of the chain length of the faster moving PS chains keeping the molecular weight of the slow PXE chain constant. Both experiments, however, were carried out at constant blend composition and therefore cannot comment on the concentration dependence predicted by eq 7. The phase diagram of the present polymer mixture is shifted at temperatures above 120 °C if the entanglement regime is reached for both components. At these high temperatures, however, the PEO chains are not chemically stable.

Composition Dependence. The strong composition dependent $T_g(\varphi)$ of most chemically different polymer–polymer mixtures introduces ambiguities in the analysis of the desired $D^0(\varphi)$ dependence. In the common Williams–Landel–Ferry (WLF) equation[27] widely used to represent the non-Arrhenius temperature dependence of mobility data, besides T_g the activation parameter c_1c_2 can also vary with composition. Only if the latter is insensitive to blend composition can the actually predicted $D^0(\varphi)$ be checked at constant $T - T_g(\varphi)$.[9,22] The compensation for $T_g(\varphi)$ is even better if the tracer diffusivities D_A^0 and D_B^0 are experimentally accessible at the same blend composition as the interdiffusion D. In the present PEO/PPO blend, however, no correction for free-volume effects is needed. Both T_g and activation energy E are insensitive to composition variations as shown from the data in Figures 2, 3, and 7.

Figure 9 shows the static structure factor $S(q)$ measured at a scattering angle of 90° as a function of composition at two temperatures. As experimentally verified (Figure 5), $S(q)$ is insensitive to q variation and therefore the thermodynamic limit in eq 4 is reached for $\lambda = 488$ nm at the convenient angle of 90°. The maximum in $S(q)$ near the middle of the blend composition range is in accord with the mean-field result

$$\chi_s = [(v_A\varphi_A N_A)^{-1} + (v_B\varphi_B N_B)^{-1}]v_0/2 \qquad (17)$$

for $N_A \sim N_B$ and χ_F insensitive to concentration variations.[18] In eq 17 v_i is the volume of the monomer unit of type i (=A, B), and v_0 is the volume of the refernce unit cell in the lattice model. The structure factor $S(q)$ significantly increases with decreasing temperature toward the coexistence curve, a typical behavior for a polymer mixture with UCST. The interaction parameter χ_F computed from eq 4 and 17 is positive (~0.1 at 70 °C), decreases with increasing temperature, and is rather independent of φ in the composition range 0.2–0.7.[18] The calculated $S(0)$ using $\chi_F = 0$ is also plotted for comparison in Figure 9. Recently, positive χ_F of the same order of magnitude was reported for the PEO/PPO mixture with methoxylated end groups from small-angle neutron-scattering measurements.[28]

Figure 10 shows the variation of the interdiffusion coefficient D with the volume fraction φ_{PEO} in the mixture PEO(1000)/PPO(1025) at 70 and 100 °C. Several pertinent aspects emerge from this plot. The "thermodynamic slowing down" effect on mutual diffusion near the middle of the composition range is clearly demonstrated. This minimum in D is clearly correlated with the observed maximum in $S(q)$ (Figure 9) and is in qualitative agreement with eq 5. Similar behavior was recently reported[10] for the PEO(600)/PPO(1025) mixture where D is reduced near the middle of the composition range but now toward the region rich in the shorter PEO chain (eq 17). $D(\varphi)$ in isotopic polystyrene mixtures[14] of significantly high molecular weights also experiences a minimum due again to

unfavorable segment–segment interactions ($\chi_F > 0$).

To compare qualitatively the experimental $D(\varphi)$ with the theoretically predicted composition dependences, we need to know the tracer diffusivities of the blend components in addition to the thermodynamic factor $1/S(0)$ in eq 5. Instead of the D_i^0's, the self diffusion coefficients D_A^* and D_B^* of PEO and PPO, respectively, were obtained from pulsed-field-gradient NMR.[19] In the temperature range 60–100 °C the self-diffusion coefficients exhibit an Arrhenius temperature dependence (eq 15). For PEO(1000), $D_{0,A}^* = 4.73 \times 10^{-3}$ cm^2/s, $E_A = 6.5$ kcal/mol, and for PPO(1025), $D_{0,B}^* = 7.94 \times 10^{-3}$ cm^2/s, $E_B = 6.9$ kcal/mol. Note the closeness of these values of the activation energy with that of the mutual diffusion coefficient in dilute PEO(1000)/PPO(1025) mixtures (Figure 7). Moreover, at the same temperature the microscopic self-diffusivities w_A^* ($=D_A^* N_A$) and w_B^* ($=D_B^* N_B$) for PEO and PPO chains, respectively, have similar values; $w_A^* = 7.6 \times 10^{-6}$ cm^2/s and $w_B^* = 5.5 \times 10^{-6}$ cm^2/s at 70 °C. Parenthetically, we should add that at the same temperature the self-diffusivities D_A^* and D_B^* are greater than the interdiffusion D in the PEO/PPO mixture as expected (eq 5) for positive χ_F.[10,11] Now, as required by eq 6 and 7 w_A^0 ($=D_A^0 N_A$) and w_B^0 ($=D_B^0 N_B$) are the microscopic mobilities w_{AB}^0 and w_{BA}^0 in the limit $\varphi_A \to 0$ and $\varphi_B \to 0$, respectively.[3] It seems therefore reasonable to set the w_{AB}^0 for the motion of an A chain in a melt of B chains equal to the self-mobility w_A^* and likewise $w_{BA}^0 \approx w_B^*$.

The predictions of the slow (eq 6) and fast (eq 7) theory using the values of $S(0)$ (Figure 9) and D_A^* and D_B^* in eq 5 are shown as solid lines in Figure 10. While an agreement with the experimental D in the mixtures rich in either PEO or PPO is observed, deviations are clearly evident near the middle of the blend composition range. Owing to the closeness of the microscopic Rouse diffusivities w^* of bulk PEO and PPO, the computed composition dependence of D is very similar for both models. Before discussing the possible reasons for the remarkable deviation near $\varphi \approx 0.5$ we should comment on the agreement at the extreme composition range. From the two experimentally accessible quantities D and $S(0)$, the latter is subject to larger uncertainties in the dilute region mainly due to the weak light-scattering intensity (Figure 9). We therefore consider this first comparison of dynamic light-scattering results with self-diffusion data to be very satisfactory in the extreme concentration range. This agreement can be also taken as a strong support of the data acquisition and analysis, suggesting furthermore the applicability of the photon correlation spectroscopy to study diffusional dynamics of compatible polymer blends.

We consider next the discrepancy between computed and measured mutual diffusion D near $\varphi \approx 0.5$ in terms of the transport coefficient D^0, which is readily determined from the experimental D and $S(0)$ via eq 5. The variation of the purely dynamic factor $D^0(\varphi)$ with concentration is depicted in Figure 11. Again the predictions of eq 6 and 7 assuming composition-independent w_A^* and w_B^* are compared with the experimental results in Figure 11. Under this assumption both theoretical eq 6 and 7 imply that D^0 should change monotonically with blend composition in contradiction with the actual behavior. Within the framework of the theoretical models leading to eq 6 and 7 the enhanced mobility near $\varphi \approx 0.5$ can be explained only if w_A^0 and w_B^0 depend on blend composition.[22] This would further suggest that the microscopic friction coefficient $\zeta(\varphi)$ is reduced in the middle of the composition range probably due to specific hydrogen-bond interactions. However, the variation with composition of the apparent

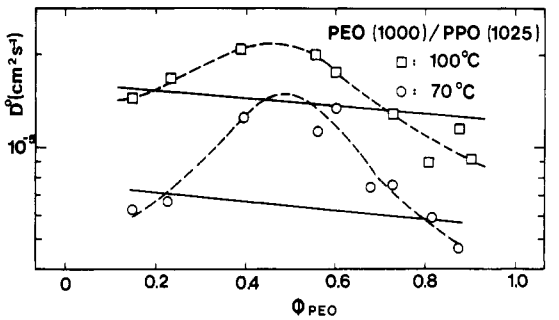

Figure 11. Transport coefficient D^0 as a function of composition φ_{PEO} for PEO(1000)/PPO(1025) blends at 100 °C (□) and 70 °C (○). Dashed lines are drawn as a guide for the eye. Solid lines are the calculated values of D^0 by inserting the self-diffusion coefficients of PEO(1000) and PPO(1025) from NMR measurements[19] into eq 6 and 7 at 100 and 70 °C.

activation energy for shear viscosity (Figure 3) cannot support a concentration-dependent ζ. Also the fact that interaction parameter χ_F is insensitive to composition variations[18] is in agreement with the lack of favored interactions near $\varphi \approx 0.5$.

We consider next the deviation from the mean-field behavior near the middle of the composition range due to its proximity to the coexistence curve. In fact the curves $S(0)$ and $D^0(\varphi)$ versus φ in Figures 9 and 11, respectively, are peculiarly similar. To check the applicability of the mean-field theory near $\varphi \approx 0.5$, we applied the Ginzburg criterion, which for a symmetrical case ($N_A = N_B$) assumes the form[29]

$$1 > \left|1 - \frac{\chi_{crit}}{\chi_F}\right| \gg 9\left(\frac{3}{4\pi}\right)^{4/3}\frac{1}{N} \tag{18}$$

where

$$\chi_{crit} = \frac{(N_B^{1/2} + N_A^{1/2})^2}{2N_A N_B} \tag{19}$$

is the critical value of χ_F corresponding to the minimum value of temperature at which the blend is still compatible. In the computations we set $N = 20$, $\chi_{crit} = 0.1$, $\chi_F = 0.09$ (100 °C), $\chi_F = 0.097$ (70 °C). We found that at 100 °C, $|1 - \chi_{crit}/\chi_F|$ is larger than twice the value of the right-hand side of inequality 18, whereas the inequality does not hold at 70 °C. If at 100 °C the difference is considered large enough to ensure applicability of the mean-field theory, then the persistence of the observed maximum of $D^0(\varphi)$ is yet to be explained. Measurements at temperatures higher than 100 °C are regrettably precluded as the PEO component becomes unstable. In this context measurements on polyisoprene–1,2-polybutadiene blends are now in progress.

Finally, deviation from the linear relation between mutual diffusion coefficient and self-diffusivities has been also observed for binary mixtures of small molecules arising from velocity cross correlations.[30] This complicated correction term was recently discussed for binary polymeric mixtures;[31] however, no exact analytical form for the interdiffusion coefficient was given. To discriminate between the two different relationships for the composition dependence of D^0, measurements of interdiffusion and static structure factor by photon correlation spectroscopy and of tracer diffusivities by other techniques (NMR, forced Rayleigh scattering) would be helpful to be conducted in dilute blends. The latter are more amenable to this study, since any complications arising from a composition dependent glass transition temperature may be considered negligible.

Conclusions

Several pertinent aspects emerge from the present photon correlation spectroscopic study of the diffusional dynamics in the poly(ethylene oxide) (PEO)/poly(propylene oxide) (PPO) mixture. The mutual diffusion coefficient D changes significantly with temperature for blend compositions near the critical concentration due to strong thermodynamic interactions. At extreme compositions, D exhibits a temperature dependence very similar to that of the shear viscosity.

At constant temperature and composition, the transport coefficient D^0 is rather insensitive to molecular weight variations, in agreement with the "fast mode" theory of mutual diffusion. The purely dynamic quantity D^0, which is a weighted average of the tracer diffusivities of the two components, can be extracted from the mutual diffusion D and the static structure factor $S(0)$ accessible from the same experiment.

At constant temperature, the mutual diffusion D in the PEO(1000)/PPO(1025) blend is strongly reduced near the middle of the composition range mainly due to the unfavorable segment–segment interactions. The positive interaction parameter χ_F leads to $D^0 < D$, in agreement with the theoretical prediction. Using the values of the self-diffusion coefficients of the blend components determined by NMR measurements, the computed values of D are in agreement with the experimental D in extreme blend compositions. However, near the middle of the composition range the φ dependence of D^0 cannot be described by either the "fast" or "slow" mode theories. Possible reasons for this discrepancy are discussed.

Acknowledgment. The financial support of the Research Center of Crete is gratefully acknowledged. Thanks are due to Dr. G. Fleischer, University of Leipzig, for providing us self-diffusion coefficients by pulsed-field-gradient NMR.

Registry No. PEO, 25322-68-3; PPO, 25322-69-4.

References and Notes

(1) de Gennes, P.-G. *Scaling Concepts in Polymer Physics*; Cornell University: Ithaca, NY, 1979.
(2) Brochard, F.; de Gennes, P.-G. *Physica A (Amsterdam)* **1983**, *118A*, 289.
(3) Binder, K. *J. Chem. Phys.* **1983**, *79*, 6387.
(4) Brereton, M. G.; Fischer, E. W.; Herkt-Maetzky, Ch.; Mortensen, K. *J. Chem. Phys.* **1987**, *87*, 6144.
(5) Akcasu, A. Z.; Benmouna, M.; Benoit, H. *Polymer* **1986**, *27*, 1935.
(6) Kramer, E. J.; Green, P. F.; Palmstrom, C. J. *Polymer* **1984**, *25*, 473.
(7) Sillescu, H. *Makromol. Chem., Rapid Commun.* **1984**, *5*, 519; **1987**, *8*, 393.
(8) Murschall, U.; Fischer, E. W.; Herkt-Maetzky, Ch.; Fytas, G. *J. Polym. Sci., Part C: Polym. Lett.* **1986**, *24*, 191.
(9) Brereton, M. G.; Fischer, E. W.; Fytas, G.; Murschall, U. *J. Chem. Phys.* **1987**, *86*, 5174.
(10) Fytas, G. *Macromolecules* **1987**, *20*, 1430.
(11) Kanetakis, J.; Fytas, G. *J. Chem. Phys.* **1987**, *87*, 5048.
(12) Composto, R. J.; Mayer, J. W.; Kramer, E. J.; White, D. M. *Phys. Rev. Lett.* **1986**, *57*, 1312.
(13) Composto, R. J.; Kramer, E. J.; White, D. M. *Nature* **1987**, *328*, 234.
(14) Green, P. F.; Doyle, B. L. *Macromolecules* **1987**, *20*, 2471.
(15) Jordan, E. A.; Ball, R. C.; McDonnald, A.; Letters, L. J.; Jones, R. A. L.; Klein, J. *Macromolecules* **1988**, *21*, 235.
(16) Binder, K.; Sillescu, H. *Encyclopedia of Polymer Science and Engineering*, 2nd ed.; Wiley: New York, in press.
(17) Garbella, R. W.; Wendorff, J. H. *Makromol. Chem.* **1988**, *189*, 2459.
(18) Fytas, G.; Kanetakis, J. *Makromol. Chem., Macromol. Symp.* **1988**, *18*, 53.
(19) Provided by Dr. G. Fleischer, Leipzig.
(20) Wang, C. H.; Fytas, G.; Lilge, D.; Dorfmuller, Th. *Macromolecules* **1981**, *14*, 1363.
(21) Cooper, D. R.; Booth, C. *Polymer* **1977**, *18*, 164.
(22) Composto, R. J.; Kramer, E. W.; White, D. M. *Macromolecules* **1988**, *21*, 2580.
(23) Rodrigo, M. M.; Cohen, C. *Macromolecules* **1988**, *21*, 2091.
(24) Rizos, A.; Fytas, G., submitted for publication in *Macromolecules*.
(25) Sevreugin, V. A.; Skirda, V. D.; Maklakov, A. I. *Polymer* **1986**, *27*, 290.
(26) Graessley, W. W. *Adv. Polym. Sci.* **1982**, *47*, 67.
(27) Ferry, J. D. *Viscoelastic Properties of Polymers*, 3rd ed.; Wiley: New York, 1980; Chapter 11.
(28) Tomlins, P. E.; Higgins, J. S. *Macromolecules* **1988**, *21*, 425.
(29) Sariban, A.; Binder, K. *J. Chem. Phys.* **1987**, *86*, 5859.
(30) Weingartner, H.; Braun, B. M. *Ber. Bunsen-Ges. Phys. Chem.* **1985**, *89*, 906.
(31) Hess, W.; Akcasu, A. Z. *J. Phys. (Les Ulis, Fr.)* **1988**, *49*, 1261.
(32) Smith, B. A.; Samulski, E. T.; Yu, L. P.; Winnik, M. A. *Macromolecules* **1985**, *18*, 1901.

Lattice Model for Crystal–Amorphous Interphases in Lamellar Semicrystalline Polymers: Effects of Tight-Fold Energy and Chain Incidence Density[1]

Sanat K. Kumar[2] and Do Y. Yoon*

IBM Almaden Research Center, 650 Harry Road, San Jose, California 95120-6099.
Received September 9, 1988; Revised Manuscript Received December 22, 1988

ABSTRACT: The partition function for polymer chains in the interphase of lamellar crystallites has been evaluated by the enumeration of the different ways of placing chain segments on a lattice. In essence, we have reformulated the earlier work of Flory, Yoon, and Dill. In the case of fully flexible chains involving no conformational energy for tight-folds, our expression for the partition function reduces to the form reported by Marqusee and Dill, who derived their partition function through probabilistic, space-filling arguments. However, the inclusion of an energy term E_t disfavoring tight-fold conformations is found to decrease significantly the fraction of regular adjacent folds and increase the thickness of the interphase. Quantitative results from our calculations are in good agreement with the Monte Carlo results of Mansfield. The effect of the chain incidence density at the crystal surface on the fraction of regular adjacent folds is also examined, and we show that both these factors are important in determining the structure of the crystal–amorphous interphase.

Introduction

Order–disorder transitions for small-molecule systems across interphases occur over distances comparable to the molecular size. However, since the extent of the phases themselves are frequently macroscopic, the interphase may essentially be ignored in the framework of classical thermodynamics of small molecules. Frequently, therefore, these interphases are idealized, following Gibbs,[3] to be

0024-9297/89/2222-3458$01.50/0 © 1989 American Chemical Society